Mine Water and the Environment (2021) 40:570–586
https://doi.org/10.1007/s10230-020-00734-2

REVIEW

Environmental Stability of Schwertmannite: A Review

Susanta Paikaray[1]

Received: 24 September 2019 / Accepted: 29 October 2020 / Published online: 25 November 2020

Abstract

Schwertmannite is sensitive to changes in geochemical, thermal, and microbial conditions. Changes in aqueous pH beyond its stability, i.e. pH 2.5–4.5, triggers its transformation to jarosite or goethite in highly acidic environments (pH ≤ 2.5), depending on the availability of jarosite-directing cations (Na^+, NH_4^+, K^+, etc.), while goethite is the common stable end product at pH > 7.5. Schwertmannite with degraded morphology can stably exist for years in oxic intermediate pH environments (pH 5.5–6.5), but the presence of trace amounts of $Fe(II)_{aq}$ yields goethite/lepidocrocite within a few hours, especially at pH ≥ 6.5. Hematite is the sole end product at ≥ 600 °C dry heating, with goethite and ferrihydrite as intermediate phases. Siderite, maghemite, and mackinawite form in anoxic microbial conditions due to dissimilatory reduction of Fe(III) and SO_4^{2-} to Fe(II) and HS^-, while orpiment forms from As(V)-rich schwertmannites. Sorbed contaminants enhance schwertmannite stability by restricting Fe(II)–Fe(III) electron transfer and microbial degradation by occupying surface sites. Although Fe(III) and sorbed ion mobilization typically has negligible effects on schwertmannite transformation, complete schwertmannite-SO_4 release is likely in extreme conditions, and in microbial $Fe(II)_{aq}$-rich media. Dissolution–reprecipitation and solid state transformation mechanisms broadly govern schwertmannite transformation.

Keywords Fe(III)–Fe(II) electron transfer · Acid mine drainage · Dissolution–reprecipitation · Thermal transformation · Acid tolerant bacteria

Introduction

Oxidative dissolution of sulfide minerals, such as pyrite (FeS_2), arsenopyrite (FeAsS), and chalcopyrite ($CuFeS_2$) on exposure to atmospheric O_2 (Eq. 1) and/or dissolved Fe^{3+} (Eq. 2) can generate the large flux of iron-sulfate-rich acidic effluents known as acid mine drainage (AMD) (Blodau 2006; Jönsson et al. 2006; Langmuir 1997; Murad and Rojik 2003, 2004; Nordstrom 1991). The Fe^{3+} driven dissolution is ≈ 2–3 times faster and generates excess acidity per unit mass of FeS_2 (Eq. 1 vs. Eq. 2), with the required Fe^{3+} being produced by oxidation of liberated Fe^{2+} (Eqs. 1 and 2), either by atmospheric O_2 (Eq. 3) or by acidophilic bacteria such as *Acidithiobacillus ferrooxidans*. Ferric oxyhydroxides and/or oxyhydroxysulfates like schwertmannite are produced by Fe^{3+} hydrolysis (Eq. 4). Rapid schwertmannite formation by a microbial pathway has been documented worldwide, which lowers both $Fe^{2+}_{(aq)}$ and $Fe^{3+}_{(aq)}$ significantly within a few meters downstream (Acero et al. 2006; Kim et al. 2002).

$$FeS_2 + 7/2O_2 + H_2O \rightarrow Fe^{2+} + 2SO_4^{2-} + 2H^+ \quad (1)$$

$$FeS_2 + 14Fe^{3+} + 8H_2O \rightarrow 15Fe^{2+} + 2SO_4^{2-} + 16H^+ \quad (2)$$

$$Fe^{2+} + 1/4O_2 + H^+ \rightarrow Fe^{3+} + 1/2H_2O \quad (3)$$

$$8Fe^{3+} + SO_4^{2-} + 14H_2O \rightarrow Fe_8O_8(OH)_6SO_4 + 22H^+ \quad (4)$$

Schwertmannite (informally known as 'yellow boy'; Brady et al. 1986; Jones et al. 2006) is a poorly crystalline iron oxyhydroxysulfate mineral (typically $Fe_8O_8(OH)_x(SO_4)_y$, 8 – x = y and 1.0 ≤ y ≤ 1.75; Bigham et al. 1990, 1994, 1996a, b; Regenspurg et al. 2004) formed in highly acidic (pH ≈ 2.8–4.5) SO_4^{2-}-rich (1000–3000 mg L^{-1}) mine waters. The SO_4^{2-} entity 'y' can extend up to 1.84 in sulfatic environments (Yu et al. 1999). Sulfate usually ranges between 0.1

Electronic supplementary material The online version of this article (https://doi.org/10.1007/s10230-020-00734-2) contains supplementary material, which is available to authorized users.

✉ Susanta Paikaray
susanta@pu.ac.in

[1] Department of Geology, Panjab University, Chandigarh 160014, India

and 15.5 wt% for synthetic and 8.5–14.1 wt% for natural specimens, whereas the iron content varies between 43.2–56.7 and 39.4–41.8 wt%, respectively (Bigham et al. 1990). Ferric hydroxide, amorphous ferric oxide, or mine drainage mineral were terms commonly used to describe this phase (Bigham and Nordstrom 2000; Murad and Rojik 2003, 2004) around AMD localities (Acero et al. 2006; Jönsson et al. 2005; Kumpulainen et al. 2007; Regenspurg et al. 2004) before its recognition as a mineral in the 1990s (Bigham et al. 1990, 1994, 1996b). Natural streams (Schwertmann et al. 1995) and acid sulfate soils (ASS) (Burton et al. 2006, 2007; Collins et al. 2010; Jones et al. 2009) also favors schwertmannite formation. Schwertmannite is usually yellowish to reddish-brown color in natural and synthetic forms, with spheroidal micromorphology with acicular spines ≈ 100 nm in length and ≈ 10 nm wide (Supplemental Fig. S1; Antelo et al. 2013; Bigham et al. 1990, 1996a; Hockridge et al. 2009; Paikaray and Peiffer 2012a; Regenspurg et al. 2004). Structurally, schwertmannite is analogous to akaganéite (β-FeOOH), sharing double corner chains of $FeO_3(OH)_3$ octahedra producing square tunnels parallel to the c-axis (Bigham et al. 1990; Caraballo et al. 2013). This is further stabilized by the presence of SO_4^{2-} oxyanions forming bidentate bridging complexes with Fe^{3+} in the structure. Structural resemblance to ferrihydrite has also been proposed by a few researchers (e.g. Loan et al. 2004).

Schwertmannite is metastable and the favorable pH window (pH ≈ 2.8–4.5) (Bigham et al. 1990; Regenspurg et al. 2004; Wang et al. 2006) determines its abundance between jarosite at the acidic SO_4^{2-}-rich end (pH < 2.2) and goethite at the alkaline (pH > 7) end (Murad and Rojik 2004; Schwertmann and Carlson 2005). Present knowledge on schwertmannite stability suggests that the nature of product formation, transformation rates, contaminant mobilization, and Fe–S electron transfer processes are significantly influenced by bacterial metabolism, temperature, organic matter (OM), $Fe(II)_{aq}$ availability, purity, etc. Goethite is the most stable end product via an acid liberating pathway (Eq. 5) which is an extremely slow process in oxic and acidic environments, requiring years to decades to form (Acero et al. 2006; Bigham et al. 1996a, b; Jönsson et al. 2005; Regenspurg et al. 2004), while alkalinity slightly accelerates the overall kinetics that still needs months to years (Knorr and Blodau 2007; Paikaray and Peiffer 2012b; Regenspurg et al. 2004; Schwertmann and Carlson 2005). Exceptionally high surface area (SSA up to 320 $m^2\ g^{-1}$; Bigham et al. 1990) and the exchangeable SO_4^{2-} fraction of schwertmannite often causes it to be enriched in As (Burton et al. 2009; Carlson et al. 2002; Fukushi et al. 2003, 2004; Paikaray et al. 2011, 2012), Cr (Regenspurg and Peiffer 2005), Cu, Pb, Zn (Antelo et al. 2013; Sidenko and Sherriff 2005; Swedlund and Webster 2001; Webster et al. 1998), and Se (Waychunas et al. 1995), which significantly enhances its stability.

$$Fe_8O_8(OH)_{8-2x}(SO_4)_x + 2xH_2O \rightarrow 8FeOOH + 2xH^+ + xSO_4^{2-} \quad (5)$$

Mine-pit lake sediments, OM-rich constructed wetland soils (Blodau 2006; Blodau and Gatzek 2006; Blodau and Peiffer 2003; Peine et al. 2000), and re-flooding of ASS wetlands (Burton et al. 2008a, 2011; Johnston et al. 2005, 2009, 2011) are subjected to O_2-deficient reducing conditions that promotes both microbial growth and Fe^{2+} enrichment. Both conditions trigger reductive dissolution of schwertmannite (Küsel and Dorsch 2000; Regenspurg et al. 2002) releasing Fe^{2+}, SO_4^{2-}, and solid bound contaminants (e.g. As) and consuming acidity (Eqs. 6 and 7). Complete dissolution and evolution of goethite and/or lepidocrocite occurs within a few hours at pH ≥ 6.5 and $cFe(II)_{aq} \geq 1$ mM (Burton et al. 2008b; Paikaray et al. 2017). However, the presence of external ions or contaminants (e.g. As, Si, SO_4^{2-}, OM), both in solution and as a solid phase, stabilize it by limiting its dissolution (Burton et al. 2008a; Collins et al. 2010; Jones et al. 2009; Paikaray et al. 2017). Schwertmannite exposed to heat (e.g. forest fires) behave differently than its aquatic response, producing hematite along with schwertmannite (Henderson and Sullivan 2010; Henderson et al. 2007, 2008).

$$Fe_8O_8(OH)_{8-2x}(SO_4)_x + (24-2x)H^+ \Leftrightarrow 8Fe^{3+} + (16-2x)H_2O + +xSO_4^{2-} \quad (6)$$

$$CH_3COOH + Fe_8O_8(OH)_6(SO)_4 + 12H^+ \rightarrow 2HCO_3^- + 8Fe^{2+} + SO_4^{2-} + 10H_2O \quad (7)$$

where CH_3COOH represents various organic electron donors, such as yeast, lactate, glucose, and humic acids.

Understanding the stability of schwertmannite in different environmental setups is still important because of global AMD sites, where schwertmannite precipitation and dissolution affects the local environment. Hence, the objective of this review is to critically integrate the current state of knowledge on schwertmannite stability behavior in different environments so that a clear outlook can be drawn on its present status and future prospects.

Stability of Schwertmannite Under Different Environmental Conditions

Acidic Environments

The presence of jarosite-directing cations (M^+), like K^+, and NH_4^+, Na^+, promote schwertmannite transformation to jarosite (Eq. 8) at acidic conditions (pH < 2.5) with or without goethite (Barham 1997; Kumpulainen et al. 2008; Sánchez-España 2017). Jarosite can also form under prolonged pH, uncontrolled aging of schwertmannite, where

pH usually drops to the jarosite domain, since schwertmannite transformation is an acid generating process (cf. Eq. 5), e.g. pH drop from 3.09 to 1.74 in 353 days (Acero et al. 2006). In the absence of M^+, goethite forms instead, while schwertmannite remains as the only initial phase at pH ≈ 3.5 (Schroth and Parnell 2005). Besides mineralogical changes, both Fe^{3+} and SO_4^{2-} are significantly released (Acero et al. 2006). Two-stage transformation kinetics govern partial conversion of schwertmannite to jarosite and goethite with time (Table 1; Fig. 1).

$$Fe_8O_8(OH)_6SO_4 \cdot 10H_2O + M^+ + SO_4^{2-} + 16H^+ \rightarrow MFe_3(SO_4)_2(OH)_6 + 5Fe^{3+} + 18H_2O \quad (8)$$

Extreme Temperature Environments

Certain localities occasionally encounter high temperature conditions due to forest fires, e.g. the ASS lowlands of Australia (Blake et al. 2012; Bradstock et al. 2006; Henderson et al. 2007, 2008). Schwertmannite usually becomes structurally unstable during such incidents (Henderson and Sullivan 2010) and transform to crystalline iron oxides, such as hematite (α-Fe_2O_3) and maghemite (γ-Fe_2O_3), e.g. hematite abundance due to fresh bushfires on the top 5 cm of wetlands in NSW, Australia (Henderson et al. 2007, 2008). In comparison, schwertmannite transforms to traces of goethite insignificantly after several years of normal atmospheric conditions (e.g. > 1362 days at ≈ 25 °C) and is better stabilized at 4 °C, with no signs

Table 1 Nature of end products form during schwertmannite transformation in highly acidic conditions

Source material	pH	Temp. (°C)	Aging time	End product	Source
SHM + *A. ferrooxidans*	≈ 2.0	36	40 days	SHM + Jr	Wang et al. (2006)
SHM + *A. ferrooxidans*		45	21 days	Jr	
SHM + *A. ferrooxidans* + 100 mM NH_4^+		36	21 days	Jr	
SHM	≈ 3.1 → 1.7	RT	148 days	Jr + Gt	Acero et al. (2006)
SHM + 10 mM $Fe(II)_{aq}$	≈ 3.5	65	1 h	SHM + Jr + Gt	Houngaloune et al. (2015a)
SHM + 50 mM $Fe(II)_{aq}$				Gt	

Note the rapidity of Gt/Jr formation by increasing the aging temperature beyond RT and in the presence of $Fe(II)_{aq}$. pH dropped from ≈ 3.1 to 1.7 in Acero et al. (2006) study

SHM schwertmannite, *Jr* jarosite

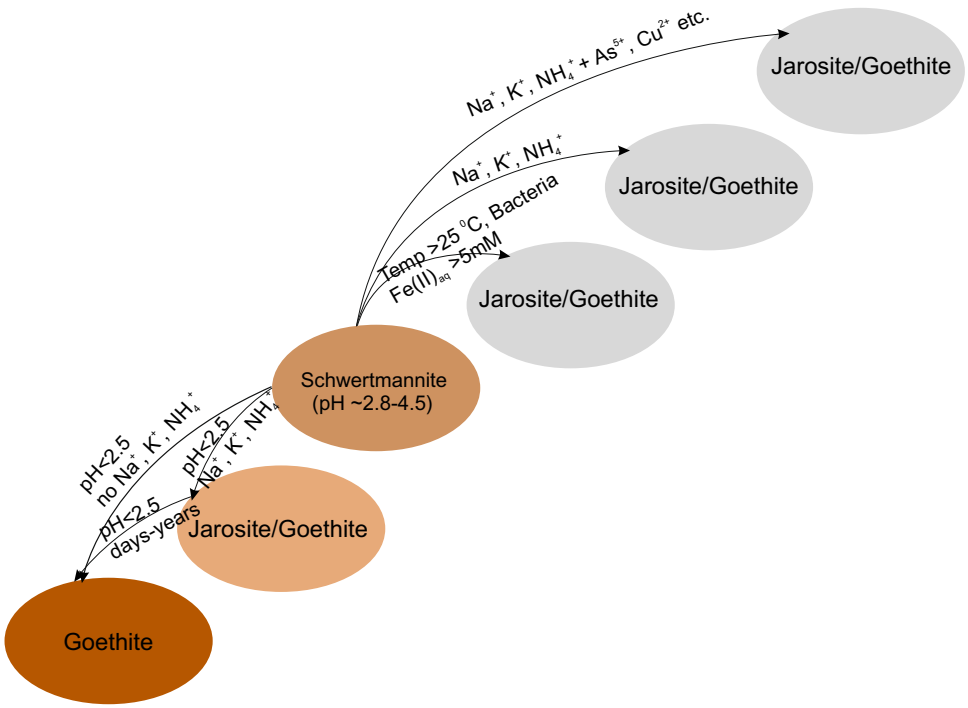

Fig. 1 Schematic diagram showing extend of schwertmannite stability and nature of end products form in acidic environments under the influence of microorganisms, temperature, contaminants and $Fe(II)_{aq}$. Note the enhanced stability by contaminants and faster transformation by $Fe(II)_{aq}$, temperature and bacteria

of transformation until ≈ 5 years (Jönsson et al. 2005). A pH drop from 3.0 to 1.9 likely triggered goethite formation in the earlier case, unlike the latter (pH ≈ 3.05 to ≈ 2.93).

Oxygenated Environments

Schwertmannite stability in oxygenated environments differs widely depending on nature (natural vs. synthetic) and purity (pure vs. trace metal enriched), exposure duration (days vs. decades), availability of foreign components (dissolved organic carbon, trace elements, etc.), pH, solid:liquid ratio, and the nature of the aqueous media (mine water vs. milli-Q water). Research data from mine drainage affected localities indicates schwertmannite predominance at pH 3.0–4.5, with goethite, ferrihydrite, and lepidocrocite at pH > 5.5, and goethite along with jarosite in acidic (pH < 2.5) conditions (Acero et al. 2005, 2006; Fukushi et al. 2003; Gagliano et al. 2004; Jönsson et al. 2005, 2006). Complete transformation of schwertmannite in O_2-rich environments usually takes months (e.g. Schwertmann and Carlson 2005; Vithana et al. 2015) to years (e.g., Kumpulainen et al. 2008) or decades, depending on the above conditions, while goethite remains the most stable end product (Bigham et al. 1996a, b; Paikaray and Peiffer 2012b; Regenspurg et al. 2004). Goethite formation is further delayed by adsorbed As and OM (Kumpulainen et al. 2008).

Anoxic Environments

Voluminous flux of OM and flooding of constructed wetlands can create anoxic conditions around mine-pit lakes (Blodau 2004; Peine et al. 2000) and ASS wetlands (Burton et al. 2006; Sullivan and Bush 2004). Dissolved O_2 is easily exhausted in AMD because of excessive Fe^{2+} ($> 10^2$–10^3 mg L^{-1}), which consumes the available O_2, and because O_2 diffusion is marginally slower in acidic environments compared to alkaline (2 vs. 4–40 cm h^{-1}) (Dempsey et al. 2001; Huang and Zhou 2012; Hustwit et al. 1992).

Anoxic, reducing environments are often rich in $Fe(II)_{aq}$ due to microbial activities that favor dissimilatory Fe(III)-reduction to $Fe(II)_{aq}$ and generation of HCO_3^- (cf. Eq. 7), which increases the pH (Burton et al. 2008b; Collins et al. 2010). Both of the parameters affected by this process, i.e. pH and $Fe(II)_{aq}$, are capable of destabilizing schwertmannite in anoxic environments and are interrelated compared to normal anoxic conditions. That means alkaline pH has negligible effects on schwertmannite stability (a time scale of days) unless the media is enriched in $Fe(II)_{aq}$, and vice versa, i.e. schwertmannite remains unchanged in the presence of elevated $Fe(II)_{aq}$ in acidic pH conditions. Studies show no mineralogical changes until 8 days in the presence of 5 mM $Fe(II)_{aq}$ at pH < 4.5 (Burton et al. 2008b), until 126 days at pH 6.5 in the absence of $Fe(II)_{aq}$ (Burton and Johnston 2012), and until ≈ 8½ days at pH 5 and 7 with 1 mM and < 1 mM $Fe(II)_{aq}$, respectively (Paikaray et al. 2017).

Controls on Schwertmannite Stability

The environmental regimes discussed above that favor schwertmannite formation can be subjected to different geochemical, microbial, and thermal variability that affect the stability of schwertmannite and which end products form. Further, the micromorphology, degree of crystallinity, SSA, proportion of mineral assemblages, etc. differ greatly, depending on the influence of various parameters (discussed below) even when the overall mineralogy of schwertmannite transformation remains the same.

pH

The most important controlling parameter of schwertmannite stability is pH. Because schwertmannite transformation is an acid-generating chemical process (Eq. 5; Acero et al. 2006; Bigham et al. 1996a), its transformation to a stable end product is expected to be the rate at which the protons (H^+) are neutralized, i.e. the supply of hydroxyl (OH^-) ions or pH of the medium. The rate at which base consumption increases determines the transformation rate with the theoretical requirement of two moles of OH^- per mole of schwertmannite (Eq. 5) or with two OH^- ions replacing one SO_4^{2-} ion (Jönsson et al. 2005). Consumption of OH^- and/or release kinetics of SO_4^{2-} are often used to estimate transformation rates (Antelo et al. 2013; Jönsson et al. 2005; Regenspurg et al. 2004) and both are well correlated (Fig. 2). Significant SO_4^{2-} release always occurs even though schwertmannite remains untransformed, which is usually reflected by $\nu_4(SO_4)$ infrared (IR) intensity (≈ 610 cm^{-1}) diminution and $\nu_3(SO_4)$ (1050 and 1130 cm^{-1}) splitting (Paikaray and Peiffer 2012b).

In acidic conditions, the rate of jarosite formation is directly proportional to the concentrations of jarosite-directing cations. Wang et al. (2006) noted that no jarosite formed until 19 and 7 days in the presence of 5.4 and 11.4 mM NH_4^+, respectively at pH ≈ 2 and 36 °C, while it was formed quickly by *A. ferrooxidans* in the presence of 165.4 mM NH_4^+. Such transformations get accelerated further by increasing aging time, temperature, and NH_4^+ concentration, whereas goethite forms in the absence of M^+ (Vithana et al. 2015); microbes like *Desulfosporosinus sp.* accelerate this process (Bertel et al. 2012).

End products like goethite and lepidocrocite form a little quicker, in a few days, when the aqueous pH is comparatively alkaline (Schwertmann and Carlson 2005) and/or acidic (Li et al. 2018), whereas schwertmannite can

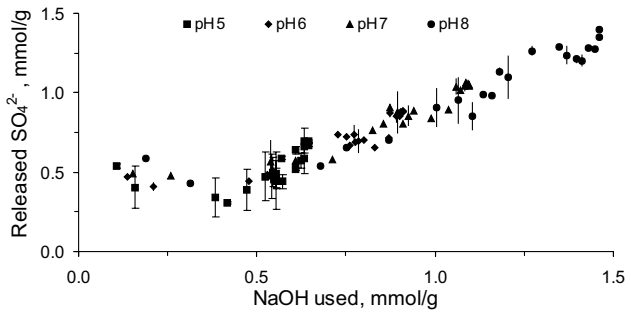

Fig. 2 Relationship between SO_4^{2-} release and OH^- consumption during the course of schwertmannite transformation under oxic condition (original source, with permission: Paikaray and Peiffer 2010)

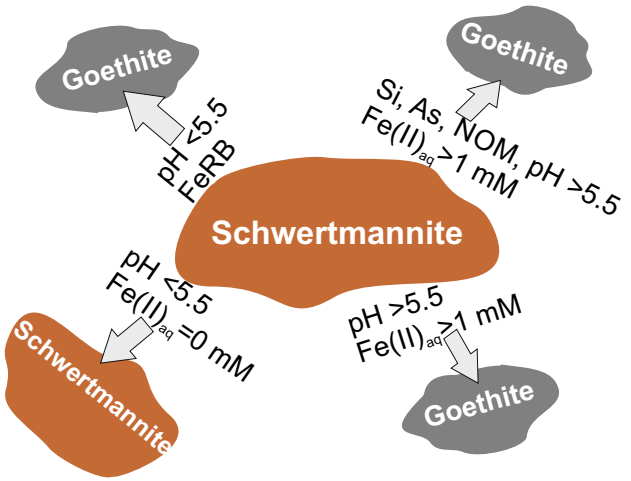

Fig. 3 A schematic diagram to illustrate the effect of pH and $Fe(II)_{aq}$ on stability of schwertmannite under anoxic conditions. Note the early formation of goethite in presence of > 1 mM $Fe(II)_{aq}$ and/or FeRB and stabilization of schwertmannite by pre-adsorbed As, Si, NOM etc.

remain unchanged for several months at pH ≈ 5 (Jönsson et al. 2006; Knorr and Blodau 2007). Under anoxic environments, the catalytic effect of $Fe(II)_{aq}$ accelerates the pH effect, producing a stable end product in a few hours (Burton et al. 2008b; Paikaray et al. 2017) through quick loss of SO_4^{2-} and weakening of Fe–S bonding (Fig. 3), while minimal transformation occurs at circumneutral pH conditions. Although schwertmannite dissolution affects SSA, it is usually not considered to be rate determining (Acero et al. 2006; Jönsson et al. 2005).

Ferrous Iron [$Fe(II)_{aq}$]

Schwertmannite transformation is more efficient at elevated $Fe(II)_{aq}$ and alkaline pH. Rapid transformation occurs by increasing $Fe(II)_{aq}$, e.g. goethite formation in 3 h at 10 mM $Fe(II)_{aq}$, but unchanged mineralogy until 8 days in the absence of $Fe(II)_{aq}$ at pH 6.5 (Burton et al. 2008b), aligning with findings by Paikaray and Peiffer (2015) and Paikaray et al. (2017). Such transformation gets amplified further when aging temperature remains above room temperature (RT) (Houngaloune et al. 2015a).

Solid and Aqueous Phase Ions

Trace Metals

Poor crystallinity and the high SSA of schwertmannite often results in trace metal enrichment (e.g. As, Zn, Mo, Cu) from mine wastes (Carlson et al. 2002; Courtin-Nomade et al. 2005; Fukushi et al. 2003; Jönsson et al. 2005; Randall et al. 1999; Swedlund and Webster 2001; Waychunas et al. 1995; Walter et al. 2003; Webster et al. 1998) making it a promising sorbent for wastewater treatment (Burton et al. 2010; Paikaray et al. 2011, 2012, 2014; Regenspurg and Peiffer 2005). The structural occupancy of trace metals and ligand exchange with surface-bound SO_4^{2-} both enhance schwertmannite stability (Burton et al. 2010; Fukushi et al. 2003; Jönsson et al. 2005; Paikaray et al. 2011, 2012). Sorbed and dissolved ions e.g. As(III), As(V), Cu, Ni, and Zn enhance schwertmannite stability remarkably (Antelo et al. 2013; Baleeiro et al. 2018; Cruz-Hermández et al. 2017; Li et al. 2018; Liao et al. 2011; Paikaray and Peiffer 2012b). Trace elements with a strong affinity always stabilize relatively better than those with poor affinity under similar conditions. Li et al. (2018) suggests that As(V) and Mo(VI) (4.6 and 6.8 wt%, respectively) stabilize schwertmannite a little better than 0.5 wt% Cr(VI), which is consistent with Khamphila et al. (2017), who found goethite after 7, 14, and 30 days from pure, 0.72 mmol g^{-1} Se(VI) and 0.31 mmol g^{-1} Cr(VI)-loaded schwertmannite, but unchanged mineralogy after 30 days for 1.02 and 0.93 mmol g^{-1} As(V) and PO_4^{3-}, respectively.

Catalytic transformation by $Fe(II)_{aq}$ is also hindered by the presence of trace elements (Burton et al. 2010; Houngaloune et al. 2015b; Paikaray and Peiffer 2015). In the case of redox pairs, such as As(V), which is sorbed better than As(III) at pH 6–7, goethite yield was limited to 6% with As(V) compared to 72% with As(III) (Burton et al. 2010). Similar enhanced stability in microbially mediated processes by *Geobacter sulfurreducens* (Cutting et al. 2012) and abiotic conditions (Zhang et al. 2016) is also noticed in producing a mixture of magnetite and goethite. Magnetite formation is indicative of substantial Fe(II) generation through dissimilatory reduction of schwertmannite-Fe(III), though possibly inefficiently, yielding magnetite that might have passivated Fe(II)-Fe(III) electron flow by forming a partial surface coating.

Sulfate and Phosphate

Excess SO_4^{2-} content in schwertmannite usually enhances its stability due to longer SO_4^{2-} desorption kinetics (Jönsson et al. 2005), even with comparable conditions. For example, schwertmannite predominates after 120 days at pH 8 (Paikaray and Peiffer 2012b), while only goethite was observed after 100 days at pH 7.2 (Schwertmann and Carlson 2005) as end products of schwertmannites with 14.7 and 11.4 wt% SO_4^{2-}, respectively. Similar behavior was also noticed for schwertmannite synthesized by biogenic processes (Liao et al. 2011) vs. inorganic vs. natural precipitates (Bigham et al. 1994; Jönsson et al. 2005), which was thought to be due to differences in schwertmannite-SO_4 content. Dissolved SO_4^{2-}, typically present in AMD, also stabilizes schwertmannite against prompt dissolution (Burton et al. 2013).

High PO_4-richness often develops PO_4 and OC-rich schwertmannite surfaces in nature that supports growth of planktonic microbes (e.g. *leptospirilium*) unlike crystalline and nutrient-free counterparts (Sánchez-España et al. 2012) facilitating development of Fe-reducing bacteria (RB; Roden and Zachara 1996). Excess PO_4^{3-} loading normally stabilizes schwertmannite for relatively long periods, e.g. up to 41 days for ≥ 400 µmol g^{-1} PO_4 vs. 5 days for no PO_4 (Schoepfer et al. 2017). However, significant schwertmannite-Fe(III) reduction took place at low PO_4 loading, yielding greigite along with goethite.

Dissolved Silica

Concentrations of Si around AMD and ASS localities are relatively high because of the abundance of aluminosilicates and proton-driven dissolution of clay minerals (Collins et al. 2010; Povrovski et al. 2003; Preda and Cox 2004). Its affinity towards schwertmannite is negligible in an acidic pH, preventing its co-precipitation with schwertmannite (Burton and Johnston 2012; Jones et al. 2009), but in alkaline and circumneutral pH conditions, Si can form a single surface layer Langmuir absorption isotherm on schwertmannite (Burton and Johnston 2012). X-ray absorption spectroscopic study demonstrates that adsorption of Si reduces iron double-corner linkage during Fe(III) hydrolysis, thereby decreasing Fe polymerization (Doelsch et al. 2000) and enhancing its stability.

Microbial transformation is hardly affected by the presence of Si (Burton and Johnston 2012), especially when Fe(II)-schwertmannite interaction occurs prior to formation of surface-passivating Si species. Both the Fe(III) and SO_4 in the schwertmannite are microbially reduced, facilitating formation of siderite ($FeCO_3$) and mackinawite (FeS). Predominance of schwertmannite was documented after 100 years of artificial drainage of acidified coastal lowland from NE New South Wales, Australia, where Si concentrations were relatively high (< 1.8 mM) compared to $Fe(II)_{aq}$ (≈ 1 mM) and not favorable for biological reduction process (Collins et al. 2010). Such contradictory stability behavior of schwertmannite is attributed to the time of interaction, i.e. simultaneous presence of schwertmannite, $Fe(II)_{aq}$, and Si (e.g. Burton and Johnston 2012) vs. schwertmannite + Si, with later stage $Fe(II)_{aq}$ (Collins et al. 2010; Jones et al. 2009). Blockage of surface sites by pre-adsorbed Si possibly enhanced schwertmannite stability in the latter scenario together with the concentration of $Fe(II)_{aq}$ itself (5 mM, Burton and Johnston (2012) vs. 1 mM, Jones et al. (2009)). The ratio of Si: schwertmannite also partially regulates surface occupancy of Si for subsequent accessibility of $Fe(II)_{aq}$ for catalytic action, e.g. ≈ 100% (Jones et al. 2009) vs. 70% (Burton and Johnston 2012) Si occupancy.

Organic Matter, Depth, and Season

Natural organic matter (NOM) usually enhances schwertmannite stability in oxic conditions (Knorr and Blodau 2007) and also limits $Fe(II)_{aq}$ catalytic action (Morel and Hering 1993; Waychunas et al. 2001) by lowering SO_4^{2-} release, possibly due to blockage of surface sites. With increased depth below the surface of mine drainage flow, schwertmannite becomes unstable and goethite dominates, e.g. > 2 cm (Jiang and Chen 2005) or > 20 cm (Acero et al. 2006) or > 30 cm (Peretyazhko et al. 2009), resulting in an increased goethite: schwertmannite proportion with depth (Gagliano et al. 2004). H_3O^+-jarosite formation has been documented at increased depth in a mine pit lake water column, SW Spain (Sánchez-España et al. 2012). Minor schwertmannite was found up to 100 m (pH 2.2–3.0), after which it was converted to jarosite, releasing considerable amounts of SO_4^{2-}.

Seasonal mineralogical variations also occur. At one site, goethite was originally dominant during February, then schwertmannite for up to 2 months, and then goethite beyond that in May (Peretyazhko et al. 2009). The dominance of schwertmannite in spring after snowmelt and goethite in warmer summer seasons (Kumpulainen et al. 2007) may indicate that drying favors precipitate cementation, while limited S and H^+ diffusion prevents schwertmannite to goethite conversion. Schwertmannite was dominant with traces of goethite for two years (May 2002-July 2004) near the Lomnice mine, Czech Republic, which was attributed to the lack of alkaline stream water due to the hot, dry summer of 2003, maintaining the pH at ≈ 3.0 to 3.3 (Murad and Rojik 2003).

Temperature

High temperature expedites transformation of schwertmannite under acidic (e.g. Wang et al. 2006), alkaline (Davidson

et al. 2008), and $Fe(II)_{aq}$-enriched microbial conditions (Houngaloune et al. 2015a). Studies show goethite formation in 1 h at ≥ 10 mM $Fe(II)_{aq}$ and 65 °C, which remained as the sole end product at ≥ 50 mM $Fe(II)_{aq}$ (Houngaloune et al. 2015a), and jarosite formation in 40 days at 36 °C and pH ≈ 2, that was reduced to 21 days at 45 °C in the presence of *A. ferrooxidans sp.* (Wang et al. 2006). The temperature effect is most pronounced in highly alkaline media. For example, goethite formed in 200 min at 60 °C and pH ≈ 13.2, which was reduced to just 30 min at 80 °C, and was quickly transformed to hematite with minor goethite at ≥ 90 °C (Davidson et al. 2008). Three transformation stages can be inferred: (1) an induction period with no detectable transformed products, (2) a primary crystallization period of two-line (2L) ferrihydrite, goethite, and/or hematite formation, and (3) a secondary crystallization stage of 2L ferrihydrite/goethite transformation to hematite.

In addition to the effect of temperature on schwertmannite destabilization in the aqueous phase, research data suggests that dry heating beyond 600 °C is capable of producing hematite along with SO_3 gas (Hederson and Sullivan 2010; Yu et al. 2002). Stable schwertmannite up to ≈ 200 °C and its partial transformation at ≈ 400 °C followed by complete transformation to hematite at ≥ 600 °C (Hederson and Sullivan 2010; Johnston et al. 2016); hematite gains crystallinity with temperature. The OM in OM-rich schwertmannite acts as a combustion accelerant for its pyrolytic oxidation, consequently causing weight loss and a decrease in total OM content (Hederson and Sullivan 2010; Qiao et al. 2017). An extended period of thermal exposure of schwertmannite to 200–600 °C yields goethite and hematite; hematite predominates over goethite beyond 400 °C (Johnston et al. 2012). Increasing the temperature to 800 °C yields hematite much faster, e.g. in 24 h vs. 90 days at 400 °C.

2L ferrihydrite forms as an intermediate product in a few cases up to 300 °C (Qiao et al. 2017; Reichelt and Bertau 2015) but eventually transforms to hematite with better crystallinity at ≥ 500 °C, while schwertmannite predominates until ≈ 200–250 °C (Table S-1). Siderite ($FeCO_3$) and mackinawite (FeS) form together with hematite at 400 and 600 °C, becoming relatively more abundant at 600 °C, but absent at 800 °C (Johnston et al. 2012). A similar Fe(II) mineral phase, maghemite (a Fe(II)-Fe(III) oxide with a cubic spinal structure resembling magnetite), has also been detected after schwertmannite exposure to > 300–400 °C (Johnston et al. 2018). Fe(II) generation takes place through microbial reduction of schwertmannite-Fe(III) using soil OM as an electron source with initial loss of OH followed by SO_4 (Mazzetti and Thistlethwaite 2002). Intermediate phases appear between 400 and 600 °C, but disappear with time; hematite remains as the sole end product at > 800 °C (Fig. 4).

Control of Microorganisms

Both iron- and sulfur-oxidizing and -reducing bacteria are widespread in mine drainage environments and regulate their geochemistry significantly, generating acidity by promoting oxidative dissolution of Fe-sulfides (Eq. 1) or generating alkalinity by reductive dissolution of ferric (oxy)hydroxides (Eq. 9) (Nordstrom 1982; Pállová et al. 2010; Singer and Stumm 1970). Since both Fe(III) and SO_4^{2-} are readily available, schwertmannite is promptly used by both FeRB and SRB as an electron acceptor, triggering its spontaneous, reductive dissolution. Differential Fe(III) reduction capabilities are noted for few species, e.g. *G. metallireducens* and *Geobacter sp*. Inefficiently reduce schwertmannite-Fe(III), in contrast to reduction of jarosite-Fe(III) at pH 7, releasing high concentrations of Fe^{2+}, SO_4^{2-}, and K^+ (Jones et al. 2006).

Peine et al. (2000) found that the schwertmannite that was dominant at the surface layer of an acidic lake in eastern Germany abruptly transformed to goethite within 5 cm of the sediment–water interface (Fig. 5). This transformation was associated with a pH increase from ≈ 3 to ≈ 6, together with increased Fe^{2+} and SO_4^{2-} down depth, which is attributed to bacterial reduction of schwertmannite-Fe(III). The re-oxidation of Fe(II) to Fe(III) triggered formation of goethite, but SO_4^{2-} reduction is not feasible at a pH < 5.5 (Fortin et al. 1996; Blodau 2006), though partial SO_4^{2-} reduction might have occurred as alkalinity increased with depth. Besides goethite's abundance at lower depths, $FeCO_3$, FeS, and FeS_2 also constitute minor phases (Burton et al. 2006, 2013),

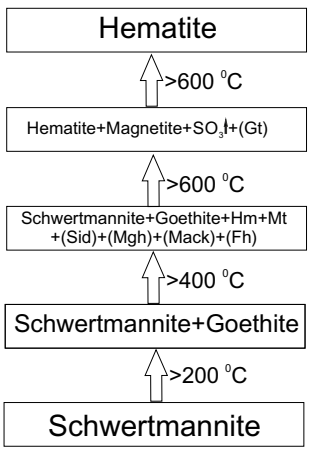

Fig. 4 The sequence of secondary phases produced from schwertmannite with respect to exposed temperature. The mineral phases are listed in decreasing abundance at any particular thermal treatment as given in each stage, while those within brackets are minor intermediate phases those may form or may not depending on the condition. SO_3 is a sulfur gas phase. *Hm* hematite, *Gt* goethite, *Fh* 2L ferrihydrite, *Mgh* maghemite, *Mt* magnetite, *Sch* schwertmannite, *Sid* siderite, *Mack* mackinawite

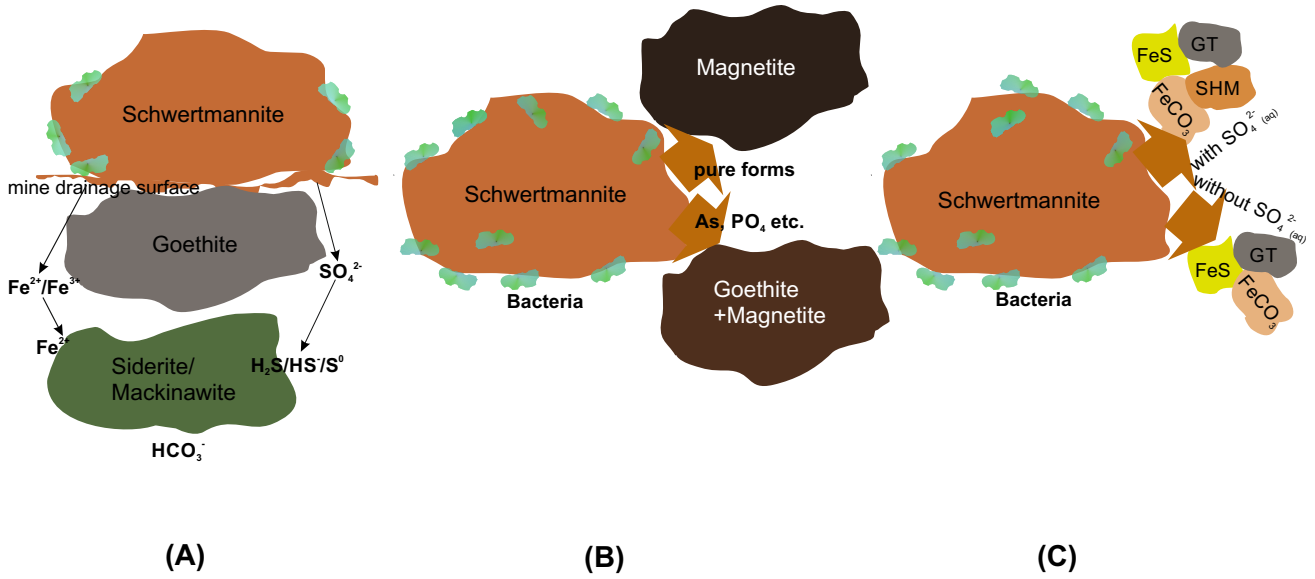

Fig. 5 Schematic diagram showing schwertmannite transformation to goethite at ≈ 5–10 cm below the mine drainage surface flow (e.g., Peine et al. 2000) where generation of Fe^{2+}/Fe^{3+} and H_2S/HS^- by FeRB and SRB can yield $FeCO_3$ and FeS (**a**). Blockage of schwertmannite surfaces by sorbed As and PO_4 for bacterial decomposition may yield goethite and magnetite contrary to magnetite yield in case of pure schwertmannite (**b**). Nature of end products form upon bacterial incubation in presence of SO_4^{2-} (**c**). Size of the individual mineral represents their approximate dominance (*Gt* goethite, *Shm* schwertmannite, *FeCO*$_3$ ferric carbonate, *FeS* mackinawite)

possibly due to dissimilatory reduction of schwertmannite-Fe(III) by FeRBs at pH ≈ 3.5, which slowly increases the pH to ≈ 6.5 (Eq. 9), favoring dissimilatory SO_4^{2-} reduction (Eq. 10). In addition to H_2S generation, partial SO_4^{2-} reduction can also produce elemental S, constituting up to 18% of the total S (Burton et al. 2013) (Eq. 11). On the other hand, Bertel et al. (2012) reported that acid-tolerant SO_4-reducing *Desulfosporosinus sp. Were* producing both FeS and Fe_3S_4 at pH 4.2 for 24 days where formation of Fe_3S_4 was more favorable at high Fe(II):Fe(III) ratios.

$$3Fe_8O_8(OH)_6SO_4 + C_6H_{12}O_6 + 6H_2O \rightarrow 24Fe^{2+} + 3SO_4^{2-} + 6CO_2 + 42OH^- \quad (9)$$

$$6H^+ + 3SO_4^{2-} + C_{12}H_{12}O_6 \rightarrow 2H_2S + 6CO_2 + 6H_2O \quad (10)$$

$$3Fe_8O_8(OH)_6SO_4 + 4H_2S + 14H^+ \rightarrow 8Fe^{2+} + 4S^0 + SO_4^{2-} + 14H_2O \quad (11)$$

Sulfur speciation along with pH variations are well reflected by XPS measurements with strong SO_4 (≈ 2481 eV) and weak elemental S (≈ 2470.6 eV) peaks in acidic media and sulfur K-edge XANES SO_4^{2-} spectra (2481 eV) along with FeS (2470 eV) (Burton et al. 2013). This reduction process is amplified when additional organic sources are available, yielding more $FeCO_3$ and FeS in expense of goethite. The pH-controlled Fe(III) (Eq. 9) and SO_4^{2-} (Eq. 10) reduction possibly governed such phase transformations, where the formed H_2S caused rapid precipitation of FeS (Eq. 12) and accumulation of Fe(II), and HCO_3^- produced $FeCO_3$ (Eq. 13). The generated $Fe(II)_{aq}$ also facilitates catalytic transformation of schwertmannite. Appearance of FeS_2 from unstable FeS is documented along anaerobic coastal lowlands (Burton et al. 2007). Reduction of As(V) in As-enriched schwertmannite yields orpiment ($As^{III}_2S_3$, Eq. 14), especially in media low in aqueous SO_4^{2-} (Burton et al. 2013).

$$Fe^{2+} + H_2S \leftrightarrow FeS + 2H^+, \quad \log K = 3.5 \quad (12)$$

$$Fe^{2+} + HCO_3^- \rightarrow FeCO_3 + H^+ \quad (13)$$

$$H_3AsO_3 + \frac{3}{2}H_2S \rightarrow \frac{1}{2}As_2S_3 + 3H_2O, \quad \log K_{orp} = 11.9 \quad (14)$$

Microbial transformation rates and nature of end products vary remarkably, depending on the nature of the initial schwertmannite and its synthesis method. Schwertmannite produced via temperature treatments up to 70 °C (SSA = 204.6 $m^2\ g^{-1}$) transformed completely to goethite in 144 h incubation with acetate, while that produced via dialysis (SSA = 159.4 $m^2\ g^{-1}$) transformed to magnetite (≈ 84%) and goethite (≈ 16%). AMD &&&sediments behave almost identically as synthetic schwertmannite under microbial domains with goethite and greigite (minor) in the presence of LNP nutrients (L = sodium lactate, N = ammonium

chloride, P = potassium dihydrogen phosphate), whereas its absence resulted in schwertmannite dominance after 100 days of incubation (Bao et al. 2018).

Nature of End Products

Schwertmannite is the predominant mineral phase in acidic mine effluents (pH 2.8–4.5) with colours of orange, brownish-yellow, and reddish-brown (Bigham et al. 1990, 1994, 1996a; Childs et al. 1998; Murad and Rojik 2003, 2004; Murad et al. 1994). Oxic and acidic environmental conditions normally witness unaffected schwertmannite for several days to years (Bigham et al. 1996a; Regenspurg et al. 2004; Schonberger 2016), as do Si- and NOM-enriched conditions in anoxic, sulfatic wetlands (Collins et al. 2010). Likewise, pre-sorbed As and the absence of any catalysts like $Fe(II)_{aq}$ yields no new products for at least a few days (Burton et al. 2008b; Johnston et al. 2016; Paikaray et al. 2017). Heating up to 200 °C also caused no mineralogical changes for several months (Johnston et al. 2016). Traces of goethite are often found to occur together with schwertmannite, possibly as a separate precipitate, being a mineral of wider stability within pH 2.5–8.5 (Bigham et al. 1990; 1996a; Murad and Rojik 2003; Yu et al. 1999). Brady et al. (1986) demonstrated that their simultaneous precipitation is possible, especially in low SO_4^{2-} mine streams with $SO_4/Fe < 1.5$. However, in a few circumstances, goethite may be a transformed product of previously precipitated schwertmannite along the stream bed (e.g. Acero et al. 2006; Schroth and Parnell 2005). The end products formed by schwertmannite transformations with different geochemical, microbial, and thermochemical setups are compiled and summarized in Fig. 6.

Ferrihydrite occurrence has been documented along the confluence of the acidic effluent (pH ≈ 3.7) from the Lomnice mine (Czech Republic) and alkaline (pH ≈ 8.4) streamwater, and further downstream (Murad and Rojik 2003). However, it was not clear whether ferrihydrite was the transformed product of schwertmannite or a direct precipitate. Its occurrence has also been noted in numerous mine drainage environments, especially at pH > 5, together with traces of goethite (Bigham et al. 1992, 1996a; Schwertmann et al. 1995; Winland et al. 1991). Precipitates of 44 AMD ochres from Australia, Finland, Germany, the U.K., and the U.S.A. suggests the abundance of schwertmannite between pH 3 and 4, ferrihydrite at pH 5–8, and goethite at pH 2.5–7.5 (Bigham et al. 1992).

Jarosite $(MFe_3(SO_4)_2(OH))_6$; $M = Na^+, K^+, NH_4^+, H_3O^+$) at pH ≤ 2.5 is evident from field and laboratory studies (e.g. Acero et al. 2006; Wang et al. 2006; Sánchez-España 2017). Prolonged aging at RT conditions, e.g. > 237 days (Acero et al. 2006) and exposure to > RT, e.g. 36 °C (40 days) and 45 °C (21 days) in the presence of jarosite directing cations was found to trigger such transformations (Wang et al. 2006).

Goethite is the most stable end product in oxic environments, requiring years to decades to form (Acero et al. 2006; Bigham et al. 1996a), while lepidocrocite and goethite forms in hours in $Fe(II)_{aq}$-enriched anoxic conditions (Burton and Johnston 2012; Burton et al. 2008b; Paikaray et al. 2017). Formation of acicular goethite is relatively fast in acidic (e.g. pH 2–3, Antelo et al. 2013; Kumpulainen et al. 2008;) and alkaline (e.g. pH 8, Kumpulainen et al. 2008) conditions, compared to near-neutral conditions (e.g. pH 5.5–6.5). The presence of trace metals, both in solid and dissolved phases (e.g. Cu(II): Antelo et al. 2013; As: Paikaray and Peiffer 2012b), enhance schwertmannite stability, but temperatures beyond RT destabilize it (Houngaloune et al. 2015a).

Anoxic microbial domains witness the formation of siderite and mackinawite due to schwertmannite-Fe(III)/SO_4 reduction (Bertel et al. 2012; Burton and Johnston 2012). Mackinawite (≈ 30%) and goethite (≈ 65%) form initially and siderite (≈ 65%) replaces goethite as the end product due to Fe(III) reduction (Burton et al. 2013). Goethite is often associated with magnetite in such scenarios, and becomes the sole end product with prolonged aging (Cutting et al. 2012; Zhang et al. 2016). Greigite (Fe_3S_4) constitutes another secondary phase in SRB media; its formation is better facilitated at higher temperature (65 °C vs. 22 °C), possibly due to faster reduction processes at higher temperatures (Burton et al. 2013). Together with $FeCO_3$ and FeS, As_2S_3 may constitute a unique phase for As(V)-rich schwertmannite (Burton et al. 2013) after dissimilatory SO_4^{2-} reduction to H_2S by SRB along with As(V) reduction to As(III) (Eq. 14).

Mobilization of Trace Metals, Fe^{3+}, and SO_4^{2-}

Mobilization of Sorbed Contaminants

Being a promising sorbent for trace metal contaminants, schwertmannite dissolution and reprecipitation as a new iron oxide/sulfide phase normally facilitate partial release of sorbed contaminants because of crystalline nature of newly formed products with poor uptake affinity (Alarcón et al. 2014; Houben 2003; Pedersen et al. 2006; Román-Ross et al. 2008). Negligible As release is frequently measured, e.g., 2 µg L^{-1} As(III) in 90 days from 9.24 wt% As(III)-schwertmannite at pH 6 and 8.5 (Liao et al. 2011); ≈ 21 µg L^{-1} (≈ 0.02%) As(III) in 154 h at pH 8 and 1 mM $Fe(II)_{aq}$ from 0.92 wt% As(III)-schwertmannite (Paikaray and Peiffer 2015). Arsenic(V) bonding onto schwertmannite is relatively stronger compared to other contaminants causing its poor release (Li et al. 2018). Similar negligible release of As (Acero et al. 2005) and Pb, Zn, Mn, As and Cu (Schroth

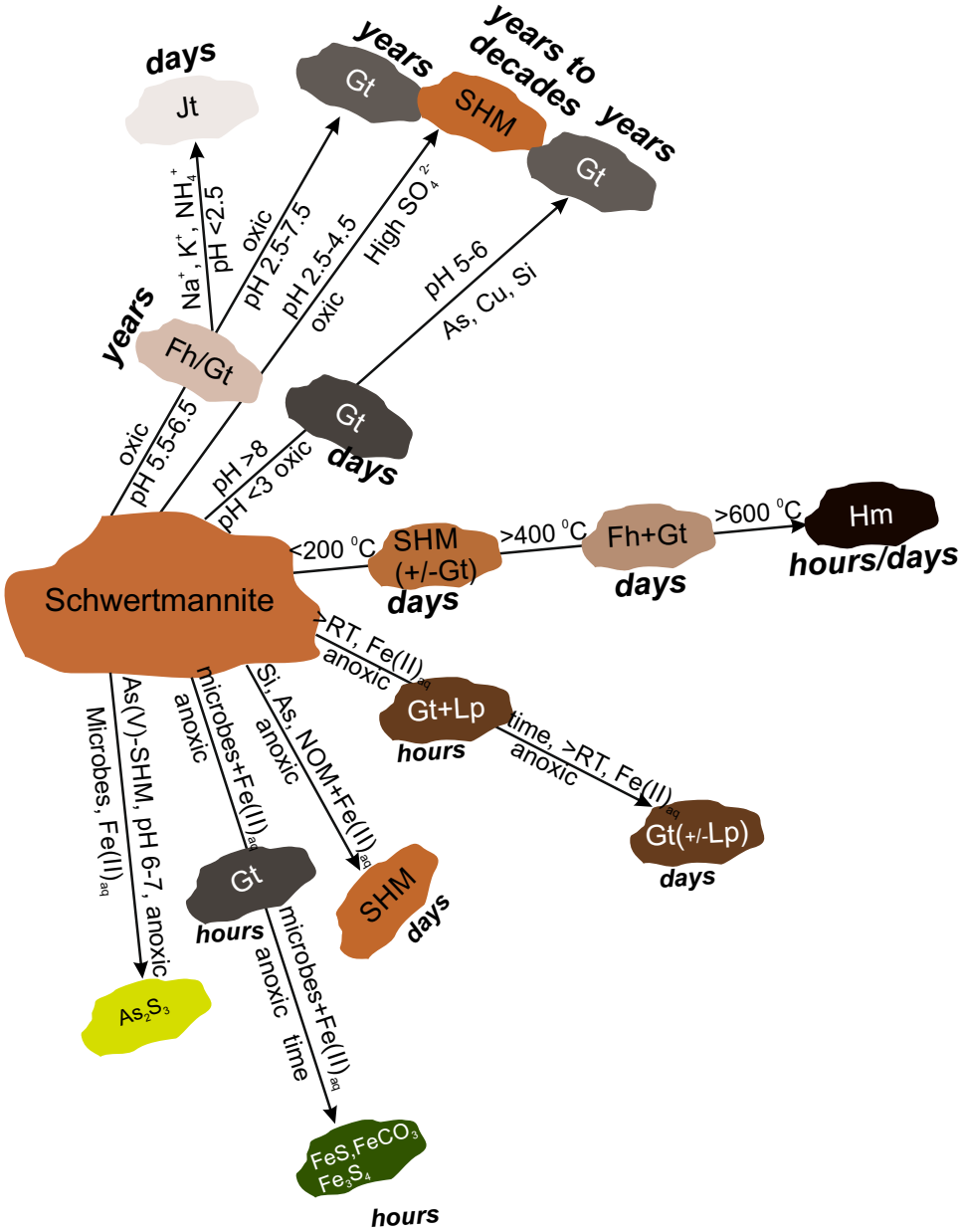

Fig. 6 A summarized chart showing nature of products form out of schwertmannite upon its exposure to different environmental conditions, e.g. oxic vs. anoxic, wetlands vs. AMD and influence of variable parameters, e.g. $Fe(II)_{aq}$, microbes, temperature, pH and contaminants. Note the differences in formed products in any particular environmental condition by varying the parameters, e.g. rapid formation of hematite with increasing temperature, goethite by increasing $Fe(II)_{aq}$, Fes, Fe_3O_4, and $FeCO_3$, by FeRB and SRB

and Parnell 2005) was also seen from naturally precipitating schwertmannites along AMD. Better fixation of Pb in jarosite structure and formation of Pb-SO_4 complexes on goethite surfaces causes Pb release negligible (Acero et al. 2006) contrary to continuous As release (21 to 791 µg L^{-1}) and unchanged Ni, Co and Cd. Besides aging time and the nature of contaminants, greater solid phase contamination normally brings greater release, e.g. 9 vs. 33 µg L^{-1} As from ≈ 0.3 vs. 4.13 wt% As(V)-schwertmannite (Cutting et al. 2012).

The aqueous pH inversely influences As release, with the highest release at pH 5 compared to pH 8 (Paikaray and Peiffer 2012b) due to readsorption of released As onto newly formed mineral phases at pH 8. The presence of competitive ions, e.g. $H_3SiO_4^-$ and SO_4^{2-} (Fig. 7a), usually enhances As release because of the strong affinity of orthosilicate (H_4SiO_4 and $H_3SiO_{4i}^-$) and polymeric Si species (Burton and Johnston 2012) and SO_4^{2-} (Burton et al. 2013) for the same sorption sites as As (Luxton et al. 2006, 2008; Swedlund and Webster 1999).

Mobilization of Schwertmannite Fe^{3+} and SO_4^{2-}

Mobilization of Fe^{3+}

Release of Fe^{3+} is negligible or sometimes nil (Paikaray and Peiffer 2015) due to its rapid precipitation as a stable ferric

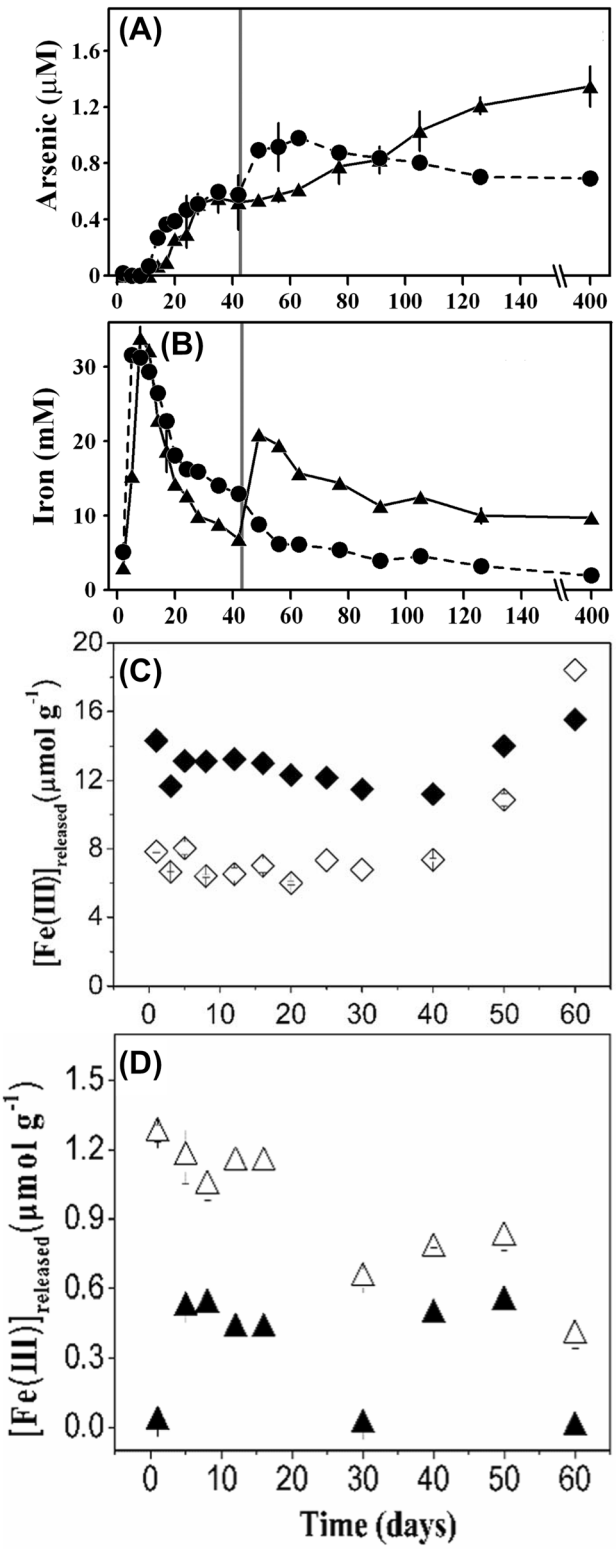

Fig. 7 Mobilization of As from schwertmannite during its transformation to stable end products in the presence of 100 mM SO_4^{2-} vs. no SO_4^{2-} (Burton et al. 2013) as a competitive ion in an aging medium. Release of Fe^{2+} during anaerobic, microbially-mediated transformation of schwertmannite (**b**) and Fe^{3+} (**c** and **d**) with schwertmannite transformation at pH 3 (**c**) and 5 (**d**) under atmospheric conditions (Li et al. 2018). The filled circles and filled triangles (**a** and **b**) represent 100 and 0 mM aqueous SO_4^{2-}, respectively, while the vertical line indicates introduction of 140 g L^{-1} glucose to the incubation system at day 43. Note that As release in 100 mM SO_4^{2-} reactors remained constant after ≈ 60 days until the completion of incubation in the 0 mM SO_4^{2-} reactors, which were also unaffected by glucose input (**a**). Likewise, note the sharp initial Fe^{2+}/Fe^{3+} release and continuous decrease thereafter (**b**, **c**, and **d**), except for a sharp Fe^{2+} release for 0 mM SO_4^{2-} after glucose input at 43 days and decrease thereafter (**b**), which suggests reprecipitation of the released iron. Also note the negligible Fe^{3+} release at pH 5 vs. pH 3 (**c** and **d**), indicative of minimal dissolution at intermediate pH and the greater Fe^{3+} release from 100 mM Cu(II) reactors (black diamond) compared to 0 mM Cu(II) (white diamond), suggestive of Cu(II)–Fe(III) association, especially at pH 3 (Li et al. 2018)

precipitate. On the other hand, rapid dissolution can initially contribute high Fe^{3+} that decreases with time (Antelo et al. 2013). Favorable dissolution under acidic pH conditions can produce up to 5 orders of magnitude greater (Fig. 7c and 7d) (Regenspurg et al. 2004; Schonberger 2016; Li et al. 2018) which is most pronounced when pH is uncontrolled (cf. Eq. 5). This can reach, for example, ≈ 1050 to ≈ 5550 mg L^{-1} in 353 days with a drop of pH from ≈ 3 to ≈ 1.7 (Acero et al. 2005, 2006) or ≈ 50 to ≈ 200 μg L^{-1} in 22 days (Schonberger 2016). The released Fe^{3+} did not reprecipitate completely, possibly because the acidic pH and/or Fe^{2+} oxidation might have partly contributed to the overall Fe^{3+} increase.

Pre-adsorbed solutes always cause relatively poor Fe^{3+} release compared to pure forms and the least release occurs in cases of highest uptake (Antelo et al. 2013; Khamphila et al. 2017). On the other hand, contaminants in the aqueous phase, e.g. Cu(II) cause more Fe^{3+} release because of their partial substitution for Fe(III) in the schwertmannite structure, provided the ionic radii are comparable (Antello et al. 2013). Ferrous iron accumulates along microbial dominated regimes that promptly respond to the availability of OM (Burton et al. 2013; Cutting et al. 2012), but are slightly lowered by SO_4^{2-} availability (Fig. 7b).

Mobilization of SO_4^{2-}

Sulfate release from schwertmannite is mostly pH dependent, with the highest amount being released at an alkaline pH, but is inhibited by pre-adsorbed sorbates such as As(III)/As(V) (Cutting et al. 2012; Paikaray and Peiffer 2012b). Replacement of schwertmannite-SO_4 by As(III) and As(V) is an important cause of excess SO_4^{2-} release (Burton et al. 2010). Greater SO_4^{2-} release always occur with As(V) exchange than As(III) because of its stronger affinity. Although goethite, the transformed product of schwertmannite, possesses substantial affinity for SO_4^{2-} under acidic conditions (Bigham et al. 1996a; Brady et al. 1986),

SO_4^{2-} release from schwertmannite can reach up to 100%; especially in highly acidic and highly alkaline conditions (Antelo et al. 2013), which remarkably modifies the overall composition of schwertmannite (Burton et al. 2008b; Jönsson et al. 2005).

The solid:water ratio (Jönsson et al. 2005), ionic strength (Jönsson et al. 2005), and aging time (Acero et al. 2005, 2006) partly controls SO_4^{2-} release. Similarly, in anaerobic environments, SO_4^{2-} release gets amplified proportionately with $Fe(II)_{aq}$ concentrations while adhering to its pH effect (Burton et al. 2008b). Likewise, alkalinity and $Fe(II)_{aq}$ combinely accelerate SO_4^{2-} release, i.e. at a constant $Fe(II)_{aq}$, more SO_4^{2-} gets released with increasing alkalinity and vice versa (Burton et al. 2008b; Houngaloune et al. 2015b). Rapid SO_4^{2-} release is often found in FeRB and SRB dominated conditions due to reductive dissolution of schwertmannite (Eq. 10), which subsequently decreases, forming Fe(II) and S(II) phases like mackinawite (Eq. 12) and siderite (Eq. 13).

Overall, three mobilization stages can be anticipated; (i) an initially rapid release of both Fe^{3+} and SO_4^{2-} when the rate of dissolution is faster than the rate of reprecipitation, followed by (ii) simultaneous dissolution and reprecipitation, and finally, (iii) negligible release of both ions (Acero et al. 2006; Antelo et al. 2013).

6. Mechanism of Schwertmannite TransformationGoethite, lepidocrocite, hematite, magnetite, mackinawite, siderite, and jarosite are common end products formed by schwertmannite transformation with(out) formation of intermediate ferrihydrite under suitable conditions. These end products themselves transform from one form to the other with time to reach the most stable form, e.g. early formation of ferrihydrite that subsequently transforms to goethite or goethite to hematite depending on the conditions of exposure. Two mechanisms govern schwertmannite transformation to stable crystalline end products, i.e. dissolution–reprecipitation and solid state transformation (Fig. 8). In the dissolution–reprecipitation mechanism, the most common process under normal atmospheric conditions, schwertmannite undergoes dissolution partially or fully depending on the geochemical variables, and a new mineral phase evolves out of the dissolved ions as a separate mineral phase, e.g. schwertmannite transforming to goethite (Burton et al. 2008a, b; Davidson et al. 2008; Paikaray and Peiffer 2012b; Paikaray et al. 2017). Suitability of goethite formation has been well documented over a wide pH range (i.e. pH 2–8, Bigham et al. 1996a) and at highly acidic and alkaline pH (i.e. pH 2 vs. pH 8 (Kumpulainen et al. 2008). The intermediate formation of ferrihydrite is proposed as aggregation of ferrihydrite followed by crystallization of hematite within the aggregates, where short range dissolution and reprecipitation is most likely (Davidson et al. 2008).

Reduction of schwertmannite-Fe(III) by FeRB generates Fe^{2+} and OH^- (Eq. 9), threatening schwertmannite stability; the produced H_2S (Eq. 10) also reacts with schwertmannite-Fe(III) (Eq. 11), generating additional Fe(II) (Peiffer and Gade 2007). Catalytic transformation of schwertmannite causes rapid dissolution and reprecipitation of thermodynamically stable iron oxides like α-FeOOH and/or γ-FeOOH with very little SO_4^{2-}. This $Fe(II)_{aq}$ effect normally functions in two mechanistic steps: (1) adsorption of $Fe(II)_{aq}$ onto schwertmannite surfaces forming surface complexes between Fe(II) and schwertmannite followed by; ((2) electron transfer between Fe(II) and structural Fe(III) (Hansel et al. 2005; Williams and Scherer 2004), which ultimately leads to the breakdown of the schwertmannite structure, releasing solid phase Fe(III), structural Fe(II), and SO_4^{2-}. The released Fe(III) immediately hydrolyzes and reprecipitates as a new phase, while the released Fe(II) re-adsorbs onto schwertmannite surfaces, continuing the dissolution process. Considering point of zero charge (pH_{PZC}) of 7.2 (Jönsson et al. 2005) or 6.6 (Regenspurg et al. 2004), greater $Fe(II)_{aq}$ absorption is expected under alkaline conditions (Houngaloune et al. 2015b), forming surface complexes on the schwertmannite surface, while no such complex forms at pH < 5 because of negligible Fe(II) adsorption (Burton et al. 2008a). However, the pH_{PZC} of iron oxides/hydroxides decrease with increases in temperature (Houngaloune et al. 2015b).

The formation of Fe-sulfide minerals like FeS and Fe_3S_4 occur in anaerobic environments through dissimilatory reduction of Fe(III) and SO_4, generating substantial Fe(II) and H_2S into the aqueous media (Burton et al. 2011, 2013; Cutting et al. 2012) where schwertmannite-SO_4/Fe(III) and released aqueous SO_4^{2-}/Fe^{3+} act as terminal electron

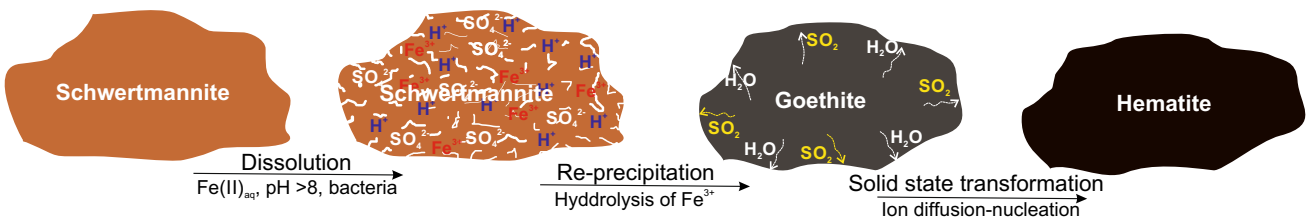

Fig. 8 Schematic representation of schwertmannite transformation mechanisms, i.e. dissolution–reprecipitation and solid state diffusion (refer to the text for detailed discussion)

acceptors for the SRB and FeRB metabolism. Their abundance in O_2-restricted AMD localities (Coupland and Johnson 2008; Pállová et al. 2010) causes simultaneous reduction of both SO_4^{2-} and Fe(III), although they compete with each other for available electron donors (Burton et al. 2008a; Lovely and Phillips 1987). Ideally, Fe(III) reduction during the course of rapid schwertmannite dissolution predominates over SO_4^{2-} reduction at pH < 5.5, while SO_4^{2-}reduction is thermodynamically more favorable at higher pH conditions (Blodau 2006; Burton et al. 2008b, 2013; Küsel et al. 1999; Regenspurg et al. 2002). However, the schwertmannite to goethite transformation often restricts Fe(III) availability for microbial action (Burton et al. 2007; Peine et al. 2000), switching the regime from Fe(III) to SO_4^{2-} reduction, making it suitable for Fe-sulfide formation (Blodau 2006; Blodau and Peiffer 2003; Burton et al. 2007, 2008a). Bacterial species of *Geobacter*, *Acidiphilium,* and *Desulfosporosinus* use schwertmannite-Fe(III) and *Desulfosporosinus*, *Desulfovibrio,* and *Desulfurispora* commonly use schwertmannite-SO_4 as electron acceptors (Bao et al. 2018). Mackinawite transformation to greigite via solid state transformation without undergoing mackinawite dissolution also partly contributes to overall greigite formation (Burton et al. 2011), while As_2S_3 formation out of As(V)-rich schwertmannite operates by the identical mechanism via simultaneous dissimilatory reduction of SO_4^{2-} to H_2S and As(V) to As(III) (Burton et al. 2013).

Simultaneous dissolution–reprecipitation and solid state transformation is possible, although a sharp distinction between the two processes is not feasible (Paikaray and Peiffer 2015). The non-uniform crystal system of schwertmannite (tetragonal) and end product lepidocrocite (orthorhombic) at RT (22 ± 2 °C) rules out complete solid state transformation. This was further supported by less SO_4^{2-} and no Fe^{3+} release in $Fe(II)_{aq}$-containing reactors (0.4–1.0 mM), compared to reactors containing no $Fe(II)_{aq}$. It would have caused excess SO_4^{2-} and Fe^{3+} release in $Fe(II)_{aq}$ reactors if dissolution–reprecipitation was the sole governing process. However, increased SO_4^{2-} release with increase in $Fe(II)_{aq}$ suggests that dissolution was active together with lepidocrocite reprecipitation. Further, being the study pH of 8 is close to the pH_{PZC} of 7.2 for schwertmannite (Jönsson et al. 2005) and $Fe(OH)_2^0$ is the predominant species at pH ≥ 7.4, the solid-state transformation process is favored.

Pre-adsorbed and/or solution phase Si (Burton and Johnston 2012; Jones et al. 2009), As (Burton et al. 2010; Paikaray and Peiffer 2012b, 2015; Paikaray et al. 2017), Cu (Houngaloune et al. 2015b), Cr (Regenspurg et al. 2004), SO_4 (Burton et al. 2013) etc. significantly enhance schwertmannite stability even under $Fe(II)_{aq}$ catalyzed transformation process. Such process operates in a twofold mechanism, (i) first, adsorption blocks the reactive surface sites of schwertmannite, which prevents/restricts dissolution and Fe(II)-Fe(III) electron transfer, and, (ii) second, its presence either in solid or aqueous phase prevents nucleation of the formed stable crystalline mineral phase (Cornell and Schwertmann 2003; Jones et al. 2009; Paikaray et al. 2017; Pedersen et al. 2005).

Conclusions and Future Prospects

Schwertmannite stability beyond pH 2.8–4.5 is largely controlled by pH, microbial metabolism, dissolved Fe^{2+}, temperature and availability of dissolved and adsorbed ions such as As, Cu, Mo, Cr, and PO_4. Goethite, being a stable ferric oxide with a wide environmental pH range (2.6–8.5), often forms in highly acidic and alkaline conditions while jarosite dominates in K^+, Na^+, and NH_4^+ enriched acidic media. Acid tolerant Fe(III)- and SO_4^{2-}-reducing bacteria such as *Geobacter* and *Desulfosporosinus* sp. and/or $Fe(II)_{aq}$ accelerate schwertmannite dissolution, releasing Fe^{2+} and H_2S into the aqueous media. This eventually yields FeS, Fe_3S_4, $FeCO_3$, maghemite, and As_2S_3 (for As(V)-rich schwertmannite) as secondary minor phases together with goethite as the dominant end product via a dissolution–reprecipitation mechanistic pathway. Surface accumulation of Fe(II) triggers Fe(II)-Fe(III) electron flow and destabilize the schwertmannite structure, ultimately causing rapid formation of goethite and ferrous sulfide minerals. However, schwertmannite can remain stable for years or decades in oxic media, especially when enriched with foreign ions such as Si, As, Cr, and contaminants with strong sorptive affinity. Although release of Fe^{3+} reaches equilibrium in a few hours with simultaneous reprecipitation as ferric oxides, significant SO_4^{2-} release occurs with schwertmannite dissolution, irrespective of oxic vs. anoxic conditions. Ligand exchange between schwertmannite-SO_4 and trace metals contributes a major fraction of overall SO_4^{2-} release, which gets amplified by FeRB/SRB activities and $Fe(II)_{aq}$ catalysis. Trace metal mobilization remains negligible and independent of schwertmannite transformation due to readsorption onto the newly formed precipitates. Most formed products follow the principle of dissolution–reprecipitation, yet solid state transformation mechanisms regulate certain conditions, especially thermal transformation beyond 400 °C.

Thus, current knowledge on schwertmannite stability provides insights to its behavior in complex environmental scenarios. However, a few specific research questions have yet to be addressed, such as the role of organic acids, differential impact of surface sorbed vs. structurally incorporated trace metals, and solar photo dissociation on its stability. Recent reports about the role of tartaric acid on its photo-reductive

dissolution exemplifies such new directions (Zhang et al. 2019). Why does the presence of H_2O accelerate thermal transformation of schwertmannite to hematite, e.g. 150 °C (Davidson et al. 2008), while it requires ≈ 400 °C with dry heat to achieve the same mineralogy (Hederson and Sullivan 2010; Johnston et al. 2012)? Although mackinawite, greigite, and siderite formation due to microbial reduction of schwertmannite-Fe(III)/SO_4 (Burton et al. 2007, 2013; Bertel et al. 2012) is confirmed, their long term stability and potential uptake of contaminants is an open question. Further, non-formation of intermediate products, such as 2L ferrihydrite, under all cases (e.g. Murad and Rojik 2004) needs better understanding. As a point of planetary interest, the discovery of schwertmannite on Mars (Bibring et al. 2007) and polar regions (Raiswell et al. 2009) opens up opportunities to establish possible environmental suitability of schwertmannite precipitation.

Acknowledgements University Grants Commission, India and Panjab University, Chandigarh, India are acknowledged for providing financial, administrative and technical support during preparation of this article. Editors and publishers of respective journals are acknowledged to provide copyright permission to reproduce selected figures. Thanks to the reviewers for their valuable inputs to improve the manuscript.

References

Acero P, Torrentó C, Ayora C (2005) Effect of schwertmannite ageing on acid rock drainage geochemistry. In: Proceedings of the 9th Int Mine Water Cong, pp 67–73

Acero P, Ayora C, Torrentó C, Nieto J (2006) The behavior of trace elements during schwertmannite precipitation and subsequent transformation into goethite and jarosite. Geochim Cosmochim Acta 70:4130–4139

Alarcón R, Gaviria J, Dold B (2014) Liberation of adsorbed and co-precipitated arsenic from jarosite, schwertmannite, ferrihydrite, and goethite in seawater. Mineral 4:603–620

Antelo J, Fiol S, Gondar D, Pérez C, López R, Arce F (2013) Cu(II) incorporation to schwertmannite: effect on stability and reactivity under AMD conditions. Geochim Cosmochim Acta 119:149–163

Baleeiro A, Fiol S, Otero-Fariña A, Antelo J (2018) Surface chemistry of iron oxides formed by neutralization of acidic mine waters: Removal of trace metals. Appl Geochem 89:129–137

Bao Y, Guo C, Lu G, Yi X, Wang H, Dang Z (2018) Role of microbial activity in Fe(III) hydroxysulfate mineral transformations in an acid mine drainage-impacted site from the Dabaoshan Mine. Sci Total Environ 616–617:647–657

Barham BJ (1997) Schwertmannite: a unique mineral, contains a replaceable ligand, transforms to jarosites, hematites, and/or basic iron sulfate. J Mater Res 12:2751–2757

Bertel D, Peck J, Quick TJ, Senko JM (2012) Iron transformations induced by an acid-tolerant *Desulfosporosinus* species. Appl Environ Microb 78:81–88

Bibring JP, Arvidson RE, Gendrin A, Gondet B, Langevin Y, Le Mouelic S, Mangold N, Morris RV, Mustard JF, Poulet F, Quantin C, Sotin C (2007) Coupled ferric oxides and sulfates on the Martian surface. Science 317:1206–1210

Bigham JM, Nordstrom DK (2000) Iron and aluminum hydroxysulfates from acid sulfate waters. In: Alpers CN, Jambor JL, Nordstrom DK (eds) Reviews in mineralogy and geochemistry, sulfate minerals: crystallography, geochemistry, and environmental significance, vol 40. Mineralogical Society of America, Washington DC, pp 351–403

Bigham JM, Schwertmann U, Carlson L, Murad E (1990) A poorly crystallized oxyhydroxysulfate of iron formed by the bacterial oxidation of Fe(II) in acid mine waters. Geochim Cosmochim Acta 54:2743–2758

Bigham JM, Schwertmann U, Carlson L (1992) Mineralogy of precipitates formed by the biogeochemical oxidation of Fe(II) in mine drainage. In: Skinner HGW. Fitzpatrick RW (Eds), Biomineralization processes of iron and manganese—modern and ancient environments. Catena Supplement Catena-Verlag, Cremlingen-Destedt, pp 219–232

Bigham JM, Carlson L, Murad E (1994) Schwertmannite, a new iron oxyhydroxysulphate from Pyhäsalmi, Finland, and other localities. Mineral Mag 58:641–648

Bigham JM, Schwertmann U, Pfab G (1996a) Influence of pH on mineral speciation in a bioreactor stimulating acid mine drainage. Appl Geochem 11:845–849

Bigham JM, Schwertmann U, Traina SJ, Winland RL, Wolf M (1996b) Schwertmannite and the chemical modeling of iron in acid sulfate waters. Geochim Cosmochim Acta 60:2111–2121

Blake D, Lu K, Horwitz P, Boyce MC (2012) Fire suppression and burnt sediments: effects on the water chemistry of fire-affected wetlands. Int J Wildland Fire 21:557–561

Blodau C (2004) Evidence for a hydrologically controlled iron cycle in acidic and iron rich sediments. Aquat Sci 66:47–59

Blodau C (2006) A review of acidity generation and consumption in acidic coal mine lakes and their watersheds. Sci Total Environ 369:307–332

Blodau C, Gatzek C (2006) Chemical controls on iron reduction in schwertmannite-rich sediments. Chem Geol 235:366–376

Blodau C, Peiffer S (2003) Thermodynamics and organic matter: constraints on neutralization processes in sediments of highly acidic waters. Appl Geochem 18:25–36

Bradstock RA, Bedward M, Cohn JS (2006) The modelled effects of differing fire management strategies on the conifer *Calltris verrucosa* within semi-arid mallee vegetation in Australia. J Appl Ecol 43:281–292

Brady KS, Bigham JM, Jaynes WF, Logan TJ (1986) Influence of sulfate on Fe-oxide formation: comparisons with a stream receiving acid mine drainage. Clays Clay Miner 34:266–274

Burton ED, Johnston SG (2012) Impact of silica on the reductive transformation of schwertmannite and the mobilization of arsenic. Geochim Cosmochim Acta 96:134–153

Burton ED, Bush RT, Sullivan LA (2006) Sedimentary iron geochemistry in acidic waterways associated with coastal lowland acid sulfate soils. Geochim Cosmochim Acta 70:5445–5468

Burton ED, Bush RT, Sullivan LA, Mitchell DRG (2007) Reductive transformation of iron and sulfur in schwertmannite-rich accumulations associated with acidified coastal lowlands. Geochim Cosmochim Acta 71:4456–4473

Burton ED, Bush RT, Sullivan LA, Mitchell DRG (2008) Schwertmannite transformation to goethite via the Fe(II) pathway: reaction rates and implications for iron-sulfide formation. Geochim Cosmochim Acta 72:4551–4564

Burton ED, Bush RT, Sullivan LA, Johnston SG, Hocking RK (2008) Mobility of arsenic and selected metals during re-flooding of iron- and organic-rich acid-sulfate soil. Chem Geol 253:64–73

Burton ED, Bush RT, Johnston SG, Watling K, Hocking RK, Sullivan LA, Heber GK (2009) Sorption of arsenic(V) and arsenic(III) to schwertmannite. Environ Sci Technol 43:9202–9207

Burton ED, Johnston SG, Watling K, Bush RT, Keene AF, Sullivan LA (2010) Arsenic effects and behavior in association with the Fe(II)-catalyzed transformation of schwertmannite. Environ Sci Technol 44:2016–2021

Burton ED, Johnston SG, Bush RT (2011) Microbial sulfidogenesis in ferrihydrite-rich environments: effects on iron mineralogy and arsenic mobility. Geochim Cosmochim Acta 75:3072–3087

Burton ED, Johnston SG, Kraal P, Bush RT, Claff S (2013) Sulfate availability drives divergent evolution of arsenic speciation during microbially mediated reductive transformation of schwertmannite. Environ Sci Technol 47:2221–2229

Caraballo MA, Rimstidt JD, Macías F, Nieto JM, Hochella MF Jr (2013) Metastability, nanocrystallinity and pseudo-solid solution effects on the understanding of schwertmannite solubility. Chem Geol 360–361:22–31

Carlson L, Bigham JM, Schwertmann U, Kyek A, Wagner F (2002) Scavenging of As from acid mine drainage by schwertmannite and ferrihydrite: a comparison with synthetic analogues. Environ Sci Technol 36:1712–1719

Childs CW, Inoue K, Mizota C (1998) Natural and anthropogenic schwertmannites from Towada-Hachimantai National Park, Honshu, Japan. Chem Geol 144:81–86

Collins RN, Jones AM, Waite TD (2010) Schwertmannite stability in acidified coastal environments. Geochim Cosmochim Acta 74:482–496

Cornell RM, Schwertmann U (2003) The iron oxides: structure, properties, reactions. Occurrences and uses. Wiley-VCH, Weinheim

Coupland K, Johnson DB (2008) Evidence that the potential for dissimilatory ferric iron reduction is widespread among acidophilic heterotrophic bacteria. FEMS Microbial Lett 279:30–35

Courtin-Nomade A, Grosbois C, Bril H, Roussel C (2005) Spatial variability of arsenic in some iron-rich deposits generated by acid mine drainage. Appl Geochem 20:383–396

Cruz-Hermández P, Peréz-López R, Nieto JM (2017) Role of arsenic during the aging of acid mine drainage precipitates. Proc Earth Planet Sci 17:233–236

Cutting RS, Coker VS, Telling ND, Kimber RL, Laan G, Pattrick RAD, Vaughan DJ, Arenholz E, Lloyd JR (2012) Microbial reduction of arsenic-doped schwertmannite by *Geobacter sulfurreducens*. Environ Sci Technol 46:12591–12599

Davidson LE, Shaw S, Benning LG (2008) The kinetics and mechanism of schwertmannite transformation to goethite and hematite under alkaline conditions. Ame Min 93:1326–1337

Dempsey BA, Roscoe HC, Ames R, Hedin R, Jeon BH (2001) Ferrous oxidation chemistry in passive abiotic systems for the treatment of mine drainage. Geochem Explor Environ Anal 1:81–88

Doelsch E, Rose J, Masion A, Bottero JY, Nohon D, Bertsch PM (2000) Speciation and crystal chemistry of iron(III) chloride hydrolysed in the presence of SiO_4 ligands. An Fe K-edge EXAFS study Langmuir 16:4726–4731

Fortin D, Davis B, Beveridge TJ (1996) Role of *Thiobacillus* and sulphate reducing bacteria in iron biocycling in oxic and acidic mine tailings. FEMS Microbiol Ecol 21:11–24

Fukushi K, Sasaki M, Sato T, Yanase N, Amano H, Ikeda H (2003) A natural attenuation of arsenic in drainage from an abandoned arsenic mine dump. Appl Geochem 18:1267–1278

Fukushi K, Sato T, Yanase N, Minato J, Yamada H (2004) Arsenate sorption on schwertmannite. Ame Miner 89:1728–1734

Gagliano WB, Brill MR, Bigham JM, Jones FS, Traina SJ (2004) Chemistry and mineralogy of ochreous sediments in a constructed mine drainage wetland. Geochim Cosmochim Acta 68:2119–2128

Hansel CM, Benner SG, Fendorf S (2005) Competing Fe(II)-induced mineralization pathways of ferrihydrite. Environ Sci Technol 39:7147–7153

Henderson SP, Sullivan LA (2010) Low temperature transformation of schwertmannite to hematite with associated CO_2, SO and SO_2 evolution. In: Proceedings of the 19th World Cong Soil Sci Soil Sol Changing World, pp 72–75

Henderson SP, Sullivan LA, Bush RT, Burton ED (2007) Schwertmannite transformation to hematite by heating: implications for pedogenesis, water quality and CO_2/SO_2 export in acid sulfate soil landscapes. Geochim Cosmochim Acta 71:A394

Henderson SP, Sullivan LA, Bush RT, Burton ED (2008) Thermal transformation of schwertmannite to hematite: anomalous stored acidity. In: Lin C, Huang S, Li Y (Eds), Proc. Joint Conf. 6th Int. Acid Sulfate Soil Conf. Acid Rock Drain. Symp., Guangzhou, China, p. 264

Hockridge JG, Jones F, Loan M, Richmond WR (2009) An electron microscopy study of the crystal growth of schwertmannite needles through oriented aggregation of goethite nanocrystals. J Cryst Growth 311:3876–3882

Houben GJ (2003) Iron incrustations in wells. Part 1: genesis, mineralogy and geochemistry. Appl Geochem 18:927–939

Houngaloune S, Hiroyoshi N, Ito M (2015a) Stability of As(V)-sorbed schwertmannite under porphyry copper mine conditions. Min Eng 74:51–59

Houngaloune S, Hiroyoshi N, Ito M (2015b) Effect of Fe(II) and Cu(II) on the transformation of schwertmannite to goethite under acidic condition. Int J Chem Eng Appl 6:32–37

Huang S, Zhou X (2012) Fe^{2+} oxidation rate drastically affect the formation and phase of secondary iron hydroxysulfate mineral occurred in acid mine drainage. Mater Sci Eng C 32:916–921

Hustwit CC, Ackman TE, Erickson PE (1992) The role of oxygen transfer in acid mine drainage (AMD) treatment. Water Environ Res 64:817–823

Johnston SG, Slavich PG, Hirst P (2005) Changes in surface water quality after inundation of acid sulfate soils of different vegetation cover. Aust J Soil Res 43:1–12

Johnston SG, Keene AF, Bush RT, Burton ED, Sullivan LA, Smith D, Martens MA, McElnea AE, Wilbraham ST, van Heel S (2009) Contemporary pedogenesis of severely degraded tropical acid sulfate soils after introduction of regular tidal inundation. Geoderma 149:335–346

Johnston SG, Keene AF, Burton ED, Bush RT, Sullivan LA (2011) Iron and arsenic cycling in intertidal surface sediments during wetland remediation. Environ Sci Technol 45:2179–2185

Johnston SG, Burton ED, Keene AF, Planer-Friedrich B, Voegelin A, Blackford MG, Lumpkin GR (2012) Arsenic mobilization and iron transformations during sulfidization of As(V)-bearing jarosite. Chem Geol 334:9–24

Johnston SG, Burton ED, Moon EM (2016) Arsenic mobilization is enhanced by thermal transformation of schwertmannite. Environ Sci Technol 50:8010–8019

Johnston SG, Bennett WW, Burton ED, Hockmann K, Dawson N, Karimian N (2018) Rapid arsenic(V)-reduction by fire in schwertmannite-rich soil enhances arsenic mobilization. Geochim Cosmochim Acta 227:1–18

Jones EJP, Nadeau T, Voytek MA, Landa ER (2006) Role of microbial iron reduction in the dissolution of iron hydroxysulfate minerals. J Geophy Res 111:1–8

Jones AM, Collins RN, Rose J, Waite TD (2009) The effect of silica and natural organic matter on the Fe(II)-catalyzed transformation and reactivity of Fe(III) minerals. Geochim Cosmochim Acta 73:4409–4422

Jönsson J, Persson P, Sjoberg S, Lovgren L (2005) Schwertmannite precipitated from acid mine drainage: phase transformation, sulphate release and surface properties. Appl Geochem 20:179–191

Jönsson J, Jönsson J, Lövgren L (2006) Precipitation of secondary Fe(III) minerals from acid mine drainage. Appl Geochem 21:437–445

Khamphila K, Kodama R, Sato T, Otake T (2017) Adsorption and post adsorption behavior of schwertmannite with various oxyanions. J Min Mater Charact Eng 5:90–106

Kim JJ, Kim SJ, Tazaki K (2002) Mineralogical characterization of microbial ferrihydrite and schwertmannite, and non-biogenic Al-sulfate precipitates from acid mine drainage in the Donghae mine area, Korea. Environ Geol 42:19–31

Knorr K, Blodau C (2007) Controls on schwertmannite transformation rates and products. Appl Geochem 22:2006–2015

Kumpulainen S, Carlson L, Raisanen ML (2007) Seasonal variations of ochreous precipitates in mine effluents in Finland. Appl Geochem 22:760–777

Kumpulainen S, Räisänen ML, Von der Kammer F, Hofmann T (2008) Ageing of synthetic and natural schwertmannites at pH 2–8. Clay Min 43:437–448

Küsel K, Dorsch T (2000) Effect of supplemental electron donors on the microbial reduction of Fe(III), sulfate, and CO_2 in coal mining-impacted freshwater lake sediments. Microb Ecol 40:238–249

Küsel K, Dorsch T, Acker G, Stackebrandt E (1999) Microbial reduction of Fe(III) in acidic sediments: Isolation of *Acidiphilium cryptum* JF-5 capable of coupling the reduction of Fe(III) to the oxidation of glucose. Appl Environ Microbiol 65:3633–3640

Langmuir D (1997) Acid mine waters. In: Mc Connin R (ed) Aqueous environmental geochemistry. Prentice-Hall, New Jersey, pp 457–478

Liao Y, Liang J, Zhou L (2011) Adsorptive removal of As(III) by biogenic schwertmannite from simulated As-contaminated groundwater. Chemosphere 83:295–301

Li J, Xie Y, Lu G, Ye H, Yi X, Reinfelder JR, Lin Z, Dang Z (2018) Effect of Cu(II) on the stability of oxyanion-substituted schwertmannite. Environ Sci Poll Res 25:15492–15506

Loan M, Cowley JM, Hart R, Parkinson GM (2004) Evidence on the structure of synthetic schwertmannite. Ame Miner 89:1735–1742

Luxton TP, Tadanier CJ, Eick MJ (2006) Mobilization of arsenite by competitive interaction with silicic acid. Soil Sci Soc Ame J 70:204–214

Luxton TP, Eick MJ, Rimstidt DJ (2008) The role of silicate in the adsorption/desorption of arsenite on goethite. Chem Geol 252:125–135

Mazzetti L, Thistlethwaite PJ (2002) Raman spectra and thermal transformations of ferrihydrite and schwertmannite. J Raman Spectrosc 33:104–111

Morel FMM, Hering JG (1993) Principles and applications of aquatic chemistry. John Wiley and Sons, New York

Murad E, Rojik P (2003) Iron-rich precipitates in a mine drainage environment: influence of pH on mineralogy. Ame Miner 88:1915–1918

Murad E, Rojik P (2004) Jarosite, schwertmannite, goethite, ferrihydrite and lepidocrocite: the legacy of coal and sulfide ore mining. In: Proceedings of the SuperSoil 2004: 3rd Australian New Zealand Soils Conference, pp 1–8

Murad E, Schwertmann U, Bigham JM, Carlson L (1994) Mineralogical characteristics of poorly crystallized precipitates formed by oxidation of Fe^{2+} in acid sulfate waters. In: Alpers CN, Blowes DW (Eds.), Environmental geochemistry of sulfide oxidation. ACS Symposium Series 550, American Chemical Society, Washington, DC, pp 190–200

Nordstrom DK (1982) Aqueous pyrite oxidation and the consequent formation of secondary iron minerals. In: Hossaer LR (ed) Acid Sulfate Weathering. Soil Sci. Soc. Amer, Madison, pp 37–63

Nordstrom DK (1991) Chemical modeling of acid mine waters in the western United States. USGS Water Res. Invest. Rep. No. 91-4034, U.S. Geol. Surv., pp 534–538

Paikaray S, Peiffer S (2010) Dissolution kinetics of sulfate from schwertmannite under variable pH conditions. Mine Water Environ 29:263–269

Paikaray S, Peiffer S (2012b) Abiotic schwertmannite transformation kinetics and the role of sorbed As(III). Appl Geochem 27:590–597

Paikaray S, Peiffer S (2012a) Biotic and abiotic schwertmannites as scavengers for As(III): mechanisms and effects. Water Air Soil Poll 223:2933–2942

Paikaray S, Peiffer S (2015) Lepidocrocite formation kinetics from schwertmannite in Fe(II)-rich anoxic alkaline medium. Mine Water Environ 34:213–222

Paikaray S, Göttlicher J, Peiffer S (2011) Removal of As(III) from acidic waters using schwertmannite: surface speciation and effect of synthesis pathway. Chem Geol 283:134–142

Paikaray S, Göttlicher J, Peiffer S (2012) As(III) retention kinetics, equilibrium and redox stability on biosynthesized schwertmannite and its fate and control on schwertmannite stability on acidic (pH 3.0) aqueous exposure. Chemosphere 86:557–564

Paikaray S, Essilfie-Dughan J, Göttlicher J, Pollock K, Peiffer S (2014) Redox stability of As(III) on schwertmannite surfaces. J Hazard Mater 265:208–216

Paikaray S, Schröder C, Peiffer S (2017) Schwertmannite stability in anoxic Fe(II)-rich aqueous solution. Geochim Cosmochim Acta 217:292–305

Pállová Z, Kupka D, Achimovičová M (2010) Metal mobilization from AMD sediments in connection with bacterial iron reduction. Miner Slov 42:343–347

Pedersen HD, Postma D, Jakobsen R, Larsen O (2005) Fast transformation of iron oxyhydroxides by the catalytic action of aqueous Fe(II). Geochim Cosmochim Acta 69:3967–3977

Pedersen HD, Postma D, Jakobsen R (2006) Release of arsenic associated with the reduction and transformation of iron oxides. Geochim Cosmochim Acta 70:4116–4129

Peine A, Küsel K, Tritschler A, Peiffer S (2000) Electron flow in an iron-rich acidic sedimant - evidence for an acidity-driven iron cycle. Limnol Oceanogr 45:1077–1087

Peretyazhko T, Zachara JM, Boily JF, Xia Y, Gassman PL, Arey BW, Burgos WD (2009) Mineralogical transformations controlling acid mine drainage chemistry. Chem Geol 262:169–178

Povrovski GS, Schott J, Farges F, Hazemann JL (2003) Iron(III)–silica interactions in aqueous solution: insights from X-ray absorption fine structure spectroscopy. Geochim Cosmochim Acta 67:3559–3573

Preda M, Cox ME (2004) Temporal variations of mineral character of acid-producing pyritic coastal sediments, Southeast Queensland, Australia. Sci Total Environ 326:257–269

Qiao X, Liu L, Shi J, Zhou L, Guo Y, Ge Y, Fan W, Liu F (2017) Heating changes bio-schwertmannite microstructure and arsenic(III) removal efficiency. Minerals 7:1–14

Raiswell R, Benning LG, Davidson L, Tranter M, Tulaczyk S (2009) Schwertmannite in wet, acid, and oxic microenvironments beneath polar and polythermal glaciers. Geology 37:431–434

Randall SR, Sherman DM, Ragnarsdottir KV, Collins CR (1999) The mechanism of cadmium surface complexation on iron oxyhydroxide minerals. Geochim Cosmochim Acta 63:2971–2987

Regenspurg S, Peiffer S (2005) Arsenate and chromate incorporation in schwertmannite. Appl Geochem 20:1226–1239

Regenspurg S, Gößner A, Peiffer S, Küsel K (2002) Potential remobilization of toxic anions during the reduction of arsenated and chromated schwertmannite by the dissimilatory Fe(III)-reducing bacterium *Acidiphilium cryptum* JF-5. Water Air Soil Poll 2:57–67

Regenspurg S, Brand A, Peiffer S (2004) Formation and stability of schwertmannite in acidic mining lakes. Geochim Cosmochim Acta 68:1185–1197

Reichelt L, Bertau M (2015) Transformation of nanostructured schwertmannite and 2-Line-ferrihydrite into hematite. Z Anorg Allg Chem 641:1696–1700

Roden EE, Zachara JM (1996) Microbial reduction of crystalline iron(III) oxides: influence of oxide surface area and potential for cell growth. Environ Sci Technol 30:1618–1628

Román-Ross G, López RP, Ayora C, Fernández A (2008) Arsenic fate during schwertmannite transformation: an EXAFS approach. Macla 9:213–214

Sánchez- España J (2017) Crystallization in acidic media: from nanoparticles to macrocrystals. Seminarios SEM Vol. 13, Sociedad Española de Mineralogía, Madrid, ISSN 1698-5478, pp 15–34

Sánchez- España J, Yusta I, López GA (2012) Schwertmannite to jarosite conversion in the water column of an acidic mine pit lake. Miner Mag 76:2659–2682

Schoepfer VA, Burton ED, Johnston SG, Kraal P (2017) Phosphate-imposed constraints 1 on schwertmannite stability under reducing conditions. Environ Sci Technol 51:9739–9746

Schonberger S (2016) Stability of schwertmannite and cobalt substituted schwertmannite in mining environments. In: Proceedings of the 29th An Symp Learn Sci through Res., pp 1–5

Schroth AW, Parnell RA (2005) Trace metal retention through the schwertmannite to goethite transformation as observed in a field setting, Alta Mine, MT. Appl Geochem 20:907–917

Schwertmann U, Carlson L (2005) The pH-dependent transformation of schwertmannite to goethite at 25°C. Clay Miner 40:63–66

Schwertmann U, Bigham JM, Murad E (1995) The first occurrence of schwertmannite in a natural stream environment. Eur J Miner 7:547–552

Sidenko NV, Sherriff BL (2005) The attenuation of Ni, Zn and Cu, by secondary Fe phases of different crystallinity from surface and ground water of two sulfide mine tailings in Manitoba, Canada. Appl Geochem 20:1180–1194

Singer PC, Stumm W (1970) Acidic mine drainage: the rate determining step. Science 167:1121–1123

Sullivan LA, Bush RT (2004) Iron precipitate accumulations associated with waterways in drained coastal acid sulfate landscapes of eastern Australia. Mar Freshw Res 55:727–736

Swedlund PJ, Webster JG (1999) Adsorption and polymerization of silicic acid on ferrihydrite, and its effect on arsenic adsorption. Water Res 33:3413–3422

Swedlund PJ, Webster JG (2001) Cu and Zn ternary surface complex formation with SO_4 on ferrihydrite and schwertmannite. Appl Geochem 16:503–511

Vithana CL, Sullivan LA, Burton ED, Bush RT (2015) Stability of schwertmannite and jarosite in an acidic landscape: Prolonged field incubation. Geoderma 239–240:47–57

Walter M, Arnold T, Reich T, Bernhard G (2003) Sorption of uranium(VI) onto ferric oxides in sulfate-rich acid waters. Environ Sci Technol 37:2898–2904

Wang H, Bigham JM, Tuovinen OH (2006) Formation of schwertmannite and its transformation to jarosite in the presence of acidophilic iron-oxidizing microorganisms. Mater Sci Eng C 26:588–592

Waychunas GA, Xu N, Fuller CC, Davis JA, Bigham JM (1995) XAS study of AsO_4^{3-} and SeO_4^{2-} substituted schwertmannites. Phys B 208–209:481–483

Waychunas GA, Jun YS, Eng PJ, Ghose SK, Trainor TP (2001) Anion sorption topology on hematite: comparison of arsenate and silicate. In: Barnett M, Kent D (eds) Developments in Earth And Environmental Sciences Vol 7—absorption of metals by Geomedia II. Elsevier, Amsterdam

Webster JG, Swedlund PJ, Webster KS (1998) Trace metal adsorption onto acid mine drainage iron(III) oxy hydroxy sulfate. Environ Sci Technol 32:1361–1368

Williams AGB, Scherer MM (2004) Spectroscopic evidence for Fe(II)-Fe(III) electron transfer at the iron oxide-water interface. Environ Sci Technol 38:4782–4790

Winland RL, Traina SJ, Bigham JM (1991) Chemical composition of ochreous precipitates from Ohio coal mine drainage. J Environ Qual 20:452–460

Yu JY, Heo B, Cho JP, Chang HW (1999) Apparent solubilities of schwertmannite and ferrihydrite in natural stream waters polluted by mine drainage. Geochim Cosmochim Acta 63:3407–3416

Yu JY, Park M, Kim J (2002) Solubilities of synthetic schwertmannite and ferrihydrite. Geochem J 36:119–132

Zhang S, Jia S, Yu B, Liu Y, Wu S, Han Xu (2016) Sulfidization of As(V)-containing schwertmannite and its impact on arsenic mobilization. Chem Geol 420:270–279

Zhang J, Li W, Li Y, Zhou L, Lan Y (2019) Tartaric acid-induced photoreductive dissolution of schwertmannite loaded with As(III) and the release of adsorbed As(III). Environ Pollut 245:711–718